IEEE Access
Multidisciplinary | Rapid Review | Open Access Journal

Received March 6, 2019, accepted March 21, 2019, date of current version May 20, 2019.

Digital Object Identifier 10.1109/ACCESS.2019.2911628

An Assessment Procedure of Distribution Network Reliability Considering Photovoltaic Power Integration

SU SU[1], YONG HU[1], LUOBIN HE[2], KOJI YAMASHITA[3], AND SHIDAN WANG[4]

[1]National Active Distribution Network Technology Research Center, Beijing Jiaotong University, Beijing 100044, China
[2]Department of Electrical Engineering, Hunan Polytechnic of Water Resources and Electric Power, Changsha 410131, Hunan, China
[3]Department of Electrical and Computer Engineering, Michigan Technological University, Houghton, MI 49931, USA
[4]State Grid Beijing Haidian Electric Power Supply Company, Beijing 100000, China

Corresponding author: Su Su (ssu@bjtu.edu.cn)

This work was supported in part by the Fundamental Research Funds for the Central Universities under Grant 2018JBM057, and in part by the National Natural Science Foundation of China under Grant 51677004.

ABSTRACT As photovoltaic (PV) generation has been one of the major renewable energy sources around the world, its PV capacity has also increased. When the large-scale PV systems are integrated into the distribution network, the complexity of the assessment process of the distribution network reliability will increase hazardously. In order to accurately assess this reliability in the distribution network combined with the PV generation, a reliability assessment procedure is proposed. In order to accurately evaluate the impact of the failure of conventional power equipment on reliability, the time-varying failure rate of conventional power equipment is modeled, taking into account the aging period. Then, in order to accurately evaluate the reliability improvement with PV systems integration, the new procedure is proposed highlighting the following contributions: 1) five new indices are added. 2) PV output is modeled so that not only the radiation intensity but also the failure and degradation of PV modules are represented. 3) time-varying islanding operation is considered and integrated. A case study using real-life distribution network topology and data in China is applied to verify that the newly proposed reliability indices display more sensitivity, and the proposed procedure significantly improves the accuracy of the reliability assessment.

INDEX TERMS Reliability assessment, distribution network, PV power integration, reliability indices, failure rate model, PV output model, islanding operation.

NOMENCLATURE

$\lambda_1(t)$	the failure rate of conventional power equipment during stabilization period
T_1	the start time of stabilization period
T_2	the start time of aging period
$\lambda_2(t)$	the failure rate of conventional power equipment during aging period
$\alpha_i(i = 1, 2)$	the shape parameter of Weibull Distribution
$\beta_i(i = 1, 2)$	the scale parameter of Weibull Distribution
SAIFI	system average interruption frequency index
SAIDI	system average interruption duration index
ASAI	average service availability index
CAIFI	customer average interruption frequency index
CAIDI	customer average interruption duration index
ENS	energy not supplied
Λ_i	annual average frequency of power outages of i-th load point
N_i	the number of electricity users of i-th load point
U_i	annual average duration of power outages of i-th load point
M_i	the number of electricity users with power outages of i-th load point
L_i	the average power of i-th load point
Λ	annual average frequency of power outages
U	annual average duration of power outages

The associate editor coordinating the review of this manuscript and approving it for publication was Shravana Musunuri.

N_t	total frequency of power outages of load point
T_{total}	total duration of power outages of load point
$YEAR$	number of years
$GRDG$	generation rate of DG
$PIPDG$	power interruption probability of DG
$PFDG$	power fluctuation of DG
$p(t)$	DG output at t moment
P_{DGN}	rated power of DG
T	total operation time of DG
$\Sigma t\{\cdot\}$	cumulative duration of a certain state
$p(t+1)$	DG output at $t+1$ moment
$APSTI$	average power supply time of island
$AESI$	average energy supplied from island
$P_{L,i}$	the load demand of i-th load point
P_{DG}	the output power of DG system
N	times of normal power supply of isolated island
R_j	the power supply area of j-th islanding operation
t_j	the power supply duration of j-th islanding operation
n	the number of data
I_i	the i–th sample of radiation intensity
$K(\cdot)$	the kernel density function
h	the bandwidth
$f_h(I)$	the probability density function of radiation intensity
P_{pvt}	the output power of PV system
P_{PVR}	the rated power of PV system under standard conditions (the radiation intensity is 1000W/m^2, and the temperature is 25°C)
I_t	the actual radiation intensity
I_0	the radiation intensity under standard conditions (the value is 1000 W/m^2)
α_P	the power-temperature coefficient of PV panel (the value is between -0.0045 and -0.0047)
T_t	the actual temperature of PV panel
T_0	the temperature under standard conditions (the value is 25°C)
T_a	the ambient temperature
$p(P)$	normal distribution function
$p(P,t)$	normal distribution function considering time variable
P	the rated power of PV modules
μ	the average power of PV modules
σ	the standard deviation of output power of PV modules
$\mu(t)$	the average power of PV modules at t moment
$\sigma(t)$	the standard deviation of output power of PV modules at t moment
P_0	the initial rated power of PV modules
A	the constant (the unit is W/year)
σ_0	the initial standard deviation of initial power of PV modules
B	the constant (the unit is W/year)
$P_{PV}(t)$	the time-varying PV output at t moment with consideration of failure and degradation of PV modules
$P_{PVt}(t)$	the time-varying PV output at t moment without consideration of failure and degradation of PV modules
η_{PVR}	the rated power coefficient of PV module
OSC	the output state coefficient of PV system
TTF	Time To Failure
TTR	Time To Repair
$U(0, 1)$	the random numbers of Uniform Distribution from 0 to 1
λ	failure rate of power equipment
μ	maintenance rate of power equipment
e	the precision
COV$(\cdot)$	the coefficient of variation
$\hat{V}(F)$	the estimated value of sample function variance
$\hat{E}(F)$	the estimated value of sample function expectation
S	the total number of samples

I. INTRODUCTION

The reliable electricity supply to the distribution network is important in terms of the national economy [1]. With the increase in photovoltaic (PV) generations, the distribution network operation becomes more challenging [2]. Compared to conventional generations, the PV output is more uncertain and intermittent, which will affect the stable power supply. Moreover, the islanding operation with the PV system may be performed when the main grid is out of service and more proper islanding operation will improve the reliability of the distribution network. Therefore, the reliability assessment of the distribution network with the PV system integration becomes of great significance.

There have been research studies in response to the reliability assessment of the distribution network, but there is still remaining work to be accomplished. The four components of literature reviews are as follows.

A. LITERATURE REVIEW ON POWER EQUIPMENT FAILURE MODELLING

The failure of conventional power equipment is a main cause of the power outage [3]. Therefore, the accuracy of the failure rate model of conventional power equipment is the key to assess the negative influence of system faults on the power supply reliability.

Many researches for the reliability assessment commonly treated the failure rate of conventional power equipment as a constant regardless of the duration of use, which means, the influence of the aging process is ignored. For example, in ref. [4], the failure rates of feeders, distribution transformers and circuit breakers were all fixed in case of the assessment of the distribution network reliability. In [5], the failure of the primary feeder was assumed to happen only at a designated time of the typical days. In [6], the constant failure rates of branches, switches, and primary substation were applied individually in the case study.

However, the failure rate of conventional power equipment is affected by the aging process and is actually time dependent [7]. The assessment results using the constant failure rate model are likely to contain a large error for the distribution network reliability. Therefore, the time-varying failure rate model for conventional power equipment is expected to improve the accuracy of the actual operation states [8].

B. LITERATURE REVIEW ON RELIABILITY INDICES

The reliability indices that were proposed by IEEE Std 1366-2012 [9] are currently widely used in the reliability assessment, which are referred to the conventional reliability indices in this paper.

The conventional reliability indices are used in [10]–[14] to analyze the distribution network reliability. However, as can be seen from the case studies in [10]–[14], the sensitivity of conventional reliability indices is quite limited.

In the case of the power outage in the main grid, the micro-grid forming an isolated network needs to solely support the local load. Therefore, the accuracy of the power supply reliability assessment in the micro-grid after the system separation becomes more important with sufficient sensitivity of the reliability indices.

Various new reliability indices that can be used to islanding operation have been proposed. In [15], the restored customer index (RCI) to reflect the restoration of electricity customers using distributed generations (DG) in islanding operation was proposed. However, RCI covers the customer' perspective only. In [16] and [17], the ''probability of purchasing electricity'' to reflect the reliability of active distribution network (ADN) from the customer's perspectives was proposed as the reliability index. The larger value denotes the poorer reliability performance especially in the case of the power outage in the main grid. However, this index can only reflect the ''probability of reliability'' instead of the specific situation of islanding operation (such as the supplied energy, etc.). In ref. [18], the micro-grid supply availability probability (MSAP) was defined for the probability of the power supply in the micro-grid. This index does not also reflect the specific situation of islanding operation. In [19], the energy served during system peak (ESSP) was proposed to assess the capability of renewable energies, i.e. an ability to supply electricity under the peak load condition. However, ESSP does not encompass the other loading conditions.

This paper proposes new reliability indices that avoid the aforementioned shortages.

C. LITERATURE REVIEW ON PV OUTPUT MODELLING

Because the radiation intensity is directly related to the PV output, the radiation intensity modelling is an essential component of the PV output model [20]. In [21], the regional and temporal distribution of solar radiation was estimated using the sunshine duration data that include the surface slope and aspect. In [22] and [23], the radiation intensity was estimated with the artificial neural network using satellite images. In [24], the segment function model of the radiation intensity was established based on geographical factors, cloud types and seasons. In [25], the concept of the global solar radiation intensity was introduced and the radiation intensity was modeled to match the historical data. In [26] and [27], the correlation between the weather/daily temperature and the solar radiation was clarified, and the radiation intensity model was established. In [28]–[30], the kernel density was estimated to establish the probability density model of radiation intensity.

The above methods are commonly used for the modeling of the PV output. However, [31]–[33] showed that the aging process of PV modules can cause the degradation of PV panels and may cause the failure of PV components including PV inverters. Therefore, actual output of PV system will be affected by the degradation and/or the failure of PV components. This point is out of scope for the current researches.

D. LITERATURE REVIEW ON RELIABILITY OF ISLANDING OPERATION

The integration of distributed generation has changed the way how to supply electricity in the distribution network. That means the main grid could coexist with the distributed generations [34]. When the main grid is out of service, the distributed generation can form the isolated grid (i.e. islanding) and attempt to maintain the power supply [35]. Therefore, the reliability of the islanding operation is important.

In [6], the system reliability with and without islanding operation in micro-grids were weighed. In [36], it is revealed that the hybrid system of biomass, PV and wind generations showed more improvement of reliability when the capacity of PV and wind generations was high. In [37], the mean available time of the distributed generation for different islanding conditions was weighed. In [38], it is emphasized that the energy storage system can improve the reliability of power supply when the wind generation is available during islanding. In [39], the influence of the success rate of islanding on the distribution network reliability was analyzed. In [40], the backtracking algorithm was proposed to detect the location (i.e. the connecting point) of the distributed generation. In [41], the fault tree method was proposed to establish the reliability model during islanding in the micro-grid, which helped to clarify the relationship between fault events and component failures. It was illustrated in [42] that the rational network structure is necessary to improve the reliability, and the fault adjacency matrix was derived in [43], which contributes more proper micro-grid structure.

Although valuable outcomes are presented in [6], [36]–[43], the power supply areas of islanding operation in [6], [36]–[43] were nearly fixed and were not dynamically changed according to the time-varying characteristics of loads and the renewable energy output. It should be noted that overgeneration can happen in the fixed power supply area of islanding operation, which means that the PV output may not be fully utilized to improve the distribution network reliability.

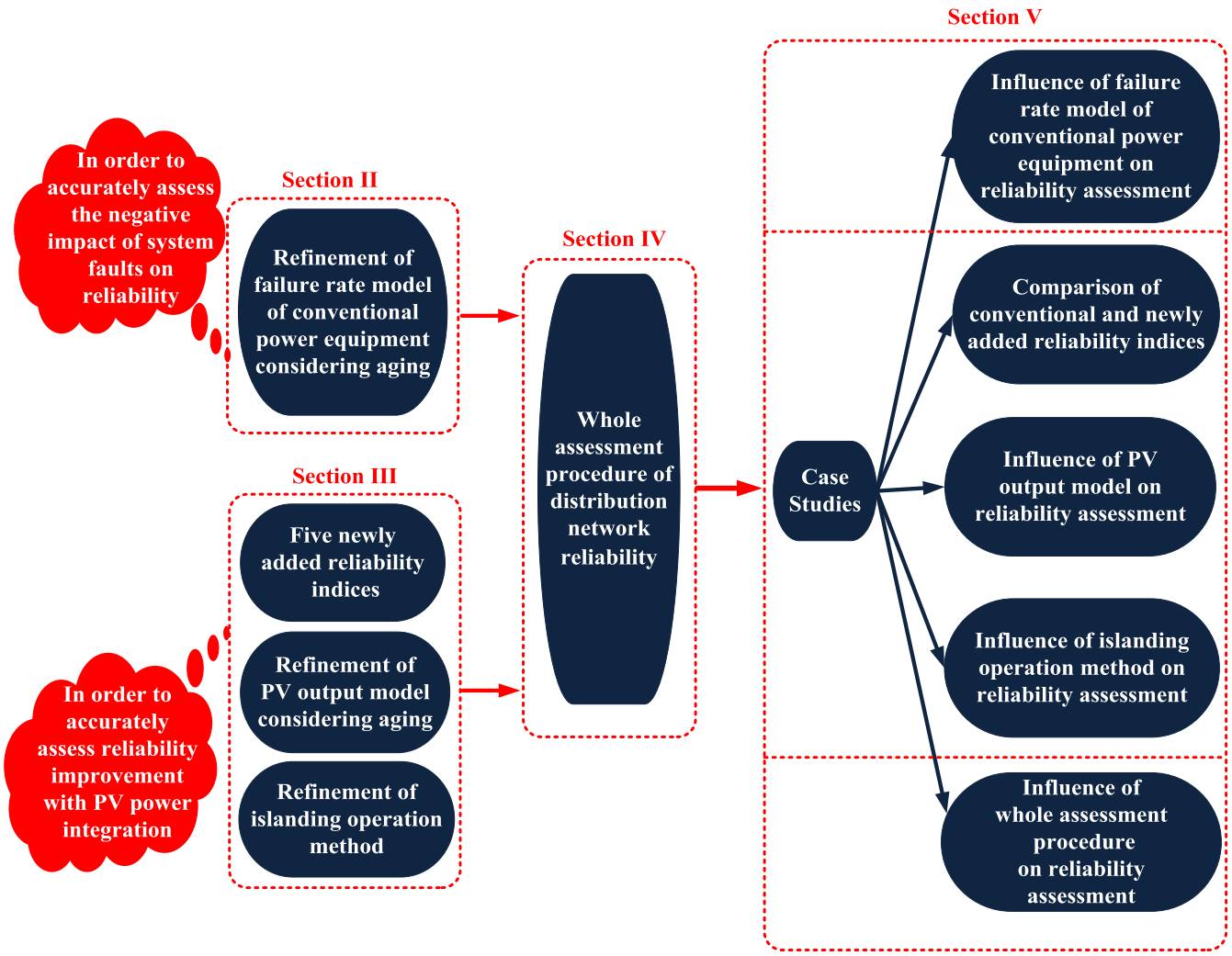

FIGURE 1. Outline of this paper.

In view of the shortages in the above aspects of the literature review, the main contributions of this paper are as follows:

(1) The failure rate model of conventional power equipment is refined in order to accurately assess the negative influence of system faults on the power supply reliability.

(2) Three items are refined in order to accurately assess the reliability improvement with PV: 1) Five reliability indices are newly added, which can ensure the sufficient sensitivity for the reliability changes in the case of the islanding operation. 2) The refined PV output model considering aging (failure and degradation of PV modules) is added. 3) The time-varying islanding operation during the power outage of main grid is considered.

(3) The whole assessment procedure is proposed.

The outline of this paper is shown in Figure 1. The rest of this paper is organized as follows:

Section II outlines the failure rate model for conventional power equipment considering aging. Section III contributes five new reliability indices, refines the PV output model considering failure and degradation of PV modules, and analyses the time-varying islanding operation. Section IV proposes the whole assessment procedure for the distribution network reliability with PV. Section V demonstrates the case studies and analyses of results. Section VI concludes the work.

II. REFINEMENT OF FAILURE RATE MODEL OF CONVENTIONAL POWER EQUIPMENT

The accuracy of the failure rate model of conventional power equipment will affect the authenticity of reliability assessment result. However, most of researches only regard the failure rate of conventional power equipment as a constant, which cannot reflect the real operation states of conventional power equipment.

The relationship between the failure rate of conventional power equipment and the operating time in its life cycle can be known as the "bathtub curve" [44], [45], which is shown in Figure 2. There are three time periods in its entire

TABLE 1. Some conventional reliability indices.

Name	Abbreviation	Calculation Equation	Unit
System Average Interruption Frequency Index	SAIFI	$SAIFI = \frac{\sum \Lambda_i N_i}{\sum N_i}$ (3)	times/ (household·year)
System Average Interruption Duration Index	SAIDI	$SAIDI = \frac{\sum U_i N_i}{\sum N_i}$ (4)	h/ (household·year)
Average Service Availability Index	ASAI	$ASAI = 1 - \frac{SAIDI}{8760}$ (5)	%
Customer Average Interruption Frequency Index	CAIFI	$CAIFI = \frac{\sum \Lambda_i N_i}{\sum M_i}$ (6)	times/ (household·year)
Customer Average Interruption Duration Index	CAIDI	$CAIDI = \frac{\sum U_i N_i}{\sum \Lambda_i N_i}$ (7)	h/ (household·year)
Energy Not Supplied	ENS	$ENS = \sum L_i U_i$ (8)	kWh/ year

life cycle: debugging period, stabilization period and aging period. In this paper, the debugging period is not considered.

During the stabilization period, the failure rate of conventional power equipment is a constant, which is given by:

$$\lambda_1(t) = \alpha_1, \quad T_1 \le t < T_2 \tag{1}$$

During the aging period, the failure rate of conventional power equipment increases as the time advances. The double Weibull Distribution is commonly used to calculate the failure rate during the aging period [45], which is given by:

$$\lambda_2(t) = \sum_{i=1}^{2} \alpha_i \beta_i t^{\beta_i - 1} = \alpha_1 + \alpha_2 \beta_2 t^{\beta_2 - 1} \tag{2}$$

III. REFINEMENT OF RELIABILITY INDICES, PV OUTPUT MODEL AND ISLANDING OPERATION

The integration of PV generations has a great potential to improve the power supply reliability of distribution network. However, 1) The calculation of conventional reliability indices involves all the load points in the distribution network, which may lead to the low sensitivity. 2) The PV system contains many components, and their aging may lead to smaller actual PV output compared to the nameplate. 3) The power supply area of the islanding operation is fixed in existing researches, which may lead to the limited use of the PV output for improving the power supply reliability.

The aforementioned three issues may make the assessment result of reliability improvement of distribution network away from the reality. When the main grid is out of service, the PV generations have to provide electricity to some load points by themselves, which puts forward higher requirements for the accuracy of the reliability assessment. Therefore, the following three refinements are studied.

A. REFINEMENT OF RELIABILITY INDICES

Representative conventional reliability indices are shown in Table 1. These reliability indices are obtained from equations (3)-(8).

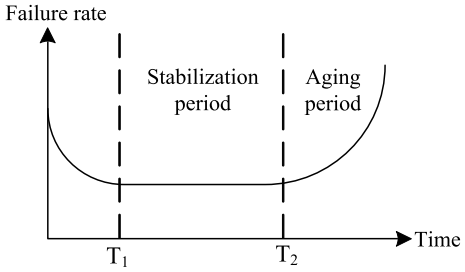

FIGURE 2. Bathtub curve model of failure rate of conventional power equipment.

In equations (3)-(8), the annual average frequency of power outages (Λ) and the annual average duration of power outages (U) can be calculated from:

$$\Lambda = \frac{N_t}{YEAR} \tag{9}$$

$$U = \frac{T_{total}}{YEAR} \tag{10}$$

As discussed in the Introduction section, the sensitivity of the conventional reliability indices is low and cannot accurately reflect the change in the reliability during the islanding operation. Thus, five reliability indices are newly added (see Table 2). The formulas for the computation of the new reliability indices are shown in equations (11)-(15). GRDG, PIPDG and PFDG aim to reflect the characteristics of PV output. APSTI and AESI focus on the power supply time and supplied energy within the area of islanding operation (i.e., R_j in equations (14)-(15)), which can ensure the sufficient sensitivity.

B. REFINEMENT OF PV OUTPUT MODEL

The aging of PV modules will lead to the failure and/or the degradation of PV modules, which will reduce the PV output. In this section, not only the time-varying radiation intensity but also the failure and the degradation of PV modules are considered to model the PV output.

TABLE 2. Newly added reliability indices.

Type	Name	Abbreviation	Calculation Equation		Unit
DG output characteristics indices	Generation Rate of DG	GRDG	$GRDG=\frac{\int_0^T p(t)dt}{P_{DGN}T}$	(11)	%
	Power Interruption Probability of DG	PIPDG	$PIPDG=\frac{\sum t\{p(t)=0\}}{T}$	(12)	%
	Power Fluctuation of DG	PFDG	$PFDG=\frac{\sum_{t=1}^{T}\lvert p(t+1)-p(t)\rvert}{T}$	(13)	W/h
Reliability indices of isolated island power supply	Average Power Supply Time of Island	APSTI	$APSTI=\frac{\sum_{j=1}^{N}t_j\{\sum_{i\in R_j}P_{L,i}<P_{DG}\}}{YEAR}$	(14)	h/ year
	Average Energy Supplied from Island	AESI	$AESI=\frac{\sum_{j=1}^{N}((\sum_{i\in R_j}P_{L,i})\cdot t_j)}{YEAR}$	(15)	kWh/ year

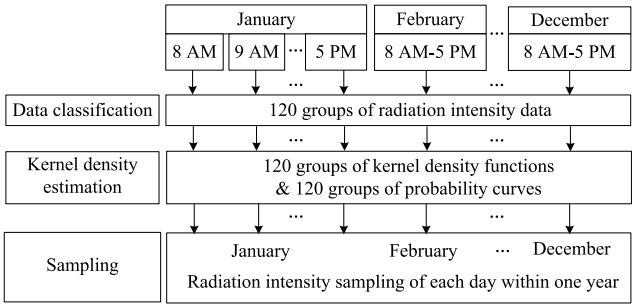

FIGURE 3. Sampling of time-varying radiation intensity.

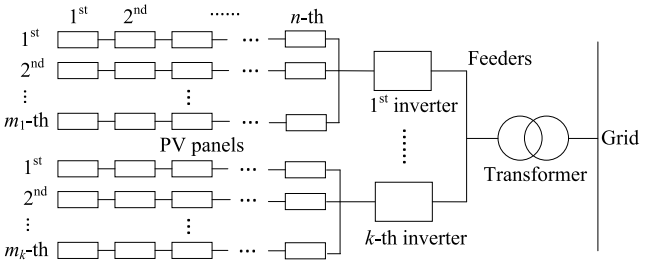

FIGURE 4. Typical structure of PV system.

1) SAMPLING OF TIME-VARYING RADIATION INTENSITY

The sampling idea for the time-varying radiation intensity is shown in Figure 3. The kernel density estimation is applied in this paper. Assuming that I_1, $I_2 \ldots I_n$ are the n samples of radiation intensity. The probability density function of the radiation intensity using the kernel density estimation is given by:

$$\hat{f}_h(I) = (1/nh) \cdot \sum_{i=1}^{n} K((I - I_i)/h), \quad -\infty < I < \infty \tag{16}$$

The historical data of the radiation intensity with the time interval of 1 hour is analyzed first. The radiation intensity data is classified into 12 groups by month. Then, the aforementioned 12 groups are further classified into 120 groups on an hourly base during 8 AM - 5 PM.

The aforementioned 120 groups of data are used to estimate the kernel density, and then 120 groups of kernel density functions and 120 groups of probability curves of kernel density are obtained.

Based on the 120 groups of kernel density estimation models, the random sampling is used to obtain the radiation intensity values of each day within one year.

The PV output model considering the radiation intensity and the temperature is given by [46]:

$$P_{\text{pvt}} = P_{PVR}(\frac{I_t}{I_0})[1 + \alpha_p(T_t - T_0)] \tag{17}$$

The temperature of PV panels depends on the ambient temperature and the radiation intensity. The actual temperature of PV panels is generally higher than the ambient temperature [46]. The actual temperature of PV panel is estimated from:

$$T_t = T_a + \frac{I_t}{1000} \cdot (\frac{T_0 - 20}{0.8}) \tag{18}$$

2) FAILURE OF PV MODULE

The PV system contains some PV panels which are connected in series and in parallel. Therefore, the failure situation of PV system will be different according to the different internal structure of PV system. The typical structure of PV system can be shown in Figure 4.

According to Figure 4, the PV system mainly consists of PV panels, inverters, feeders and a step-up transformer. n denotes the number of PV panels that are connected in series in one PV array group; $m_1 \ldots m_k$ denote the numbers of PV array groups that are connected to each inverter; k denotes the number of inverters that are connected to the grid through the transformer. Therefore, the failure of a single PV panel will only affect the PV output of this single PV array group.

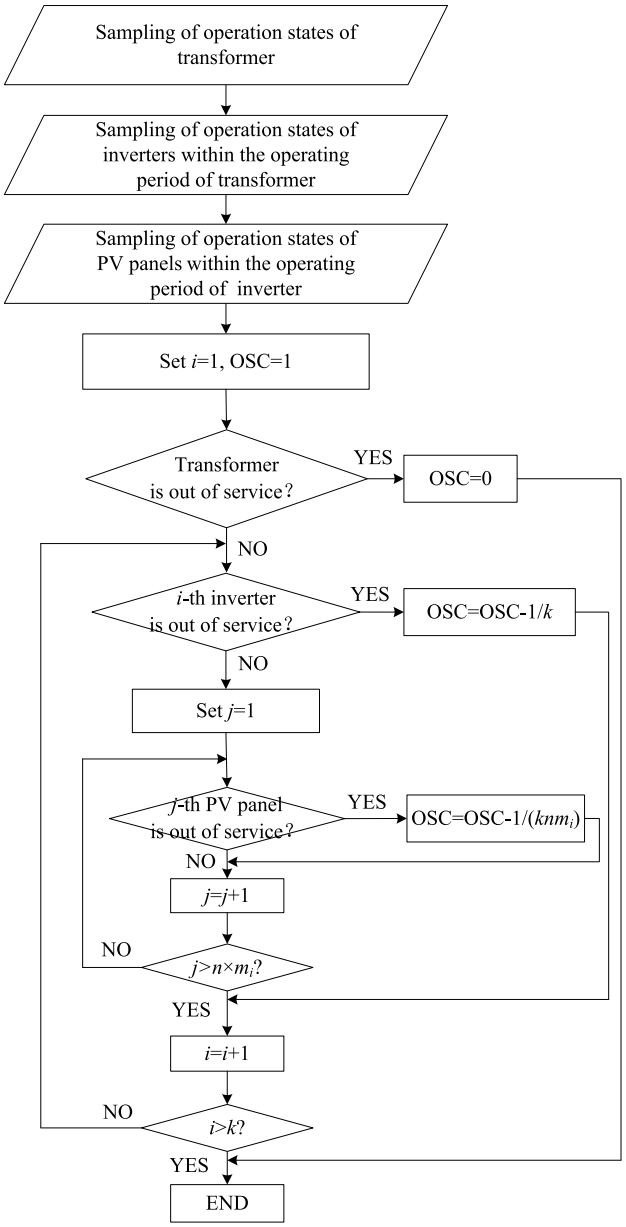

FIGURE 5. Sampling of OSC of PV system.

The failure of inverter will lead to the failure of several PV array groups. The failure of grid-connected transformer will lead to the failure of entire PV system.

In order to describe the operation states of the PV system, the output state coefficient (OSC) of the PV system is introduced. OSC is the value between 0 and 1. Specifically, 0 means that the PV system is in failure state; 1 means that the PV system is in normal operation state; the value between 0 and 1 (0 and 1 are not included) means that the PV system is in derating operation state. The sampling of OSC is shown in Figure 5. The meanings of m_i, n, and k in Figure 5 is the same as those in Figure 4.

The process of Figure 5 is described as follows. Firstly, the operation states of the transformer, inverters and PV panels

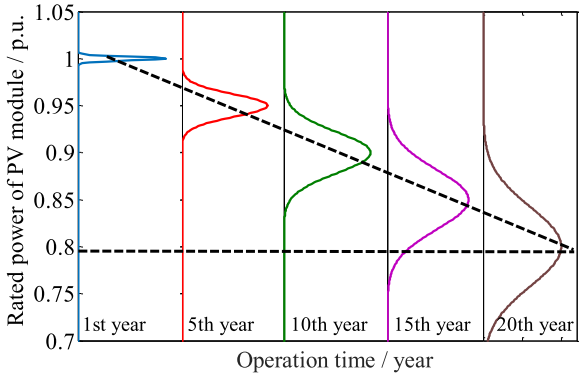

FIGURE 6. Probability density curves of degradation of PV module.

are sampled, respectively. Then, the current operation state of the transformer is judged; if the transformer is out of service, the whole system stops and the OSC is set to 0. If the transformer works normally, the current operation state of i-th inverter is judged; if i-th inverter is out of service, this PV array group does not operate. If i-th inverter works normally, the operation states of the $n \times m_i$ PV panels are judged respectively.

3) DEGRADATION OF PV MODULE

The efficiency of PV modules will gradually decrease over time. Because of this, the solar panel output follows the normal distribution [47] and the probability density function is shown by:

$$p(P) = \frac{1}{\sqrt{2\pi}\sigma} \exp[-\frac{1}{2}(\frac{P-\mu}{\sigma})^2] \tag{19}$$

The averaged solar panel output decreases almost linearly with time, which is shown by:

$$\mu(t) = P_0 - At \tag{20}$$

The standard deviation of the solar panel output also linearly varies with time, which is shown by:

$$\sigma(t) = \sigma_0 + Bt \tag{21}$$

Substituting equations (20) and (21) into equation (19), the probability density model of the degradation of the solar panel output can be obtained, which is shown by:

$$p(P,t) = \frac{1}{\sqrt{2\pi}(\sigma_0 + Bt)} \exp[-\frac{1}{2}(\frac{P-(P_0-At)}{\sigma_0+Bt})^2] \tag{22}$$

According to the statistical data of the degradation of the solar panel output, the several parameters are set as follows: A = 0.01, B = 0.002, $P_0 = 1$, $\sigma_0 = 0.002$. The probability density curves of the degradation of PV modules are shown in Figure 6. It is obvious that the average PV output gradually decreases with time, and its standard deviation gradually increases with time. After 2 decades of the operation, the averaged rated power is reduced to 80% with relative to the initial rated power, which means that the PV modules reach the expiration dates.

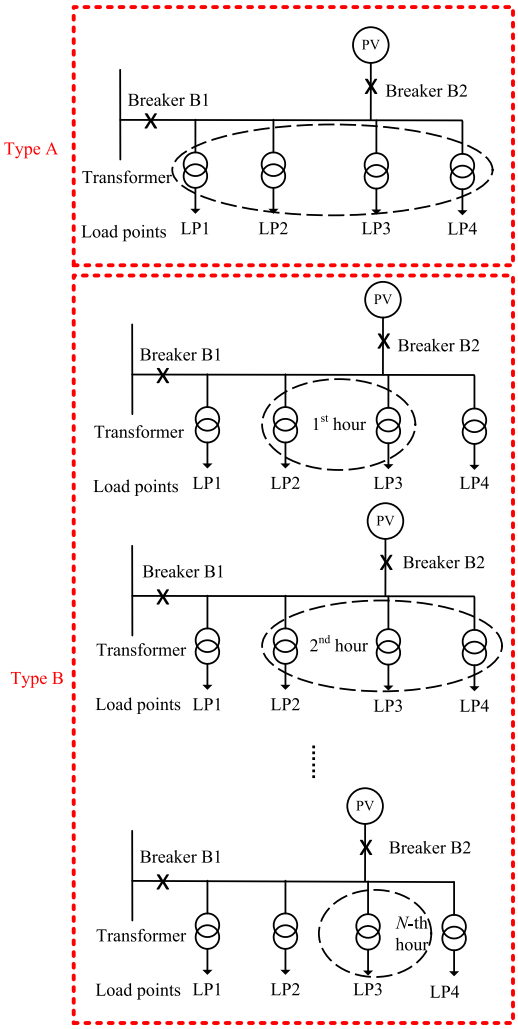

FIGURE 7. Example of two types of islanding operation.

Based on the aforementioned degradation model, the degradation rate of PV modules (which is also called the rated power coefficient of PV modules in this paper) can be obtained through sampling.

The range of degradation rate is between 0.8 and 1. Specifically, 1 means that the PV modules have no degradation, and 0.8 means that the PV modules reach the expiration date.

The actual PV output considering the failure and the degradation of PV modules is shown by:

$$P_{PV}(t) = P_{PVt}(t) \cdot \eta_{PVR} \cdot OSC \tag{23}$$

C. TIME-VARYING ISLANDING OPERATION

The PV system cannot provide the stable power output, which will have an impact on the power supply reliability. The rational utilization of the PV system can restore the power supply area as much as possible when the main grid is out of service.

Figure 7 shows an illustrative example of two types of islanding operations. As shown in Figure 7, the power supply area is fixed to LP1-LP4 in type A. When the PV output is larger than the load demand, all the load points (LP1-LP4) can be restored. On the other hand, when the PV output is lower than the load demand, the islanding operation is not performed. This type of islanding operation is simple, but it does not maximize the utilization of PV output during the system restoration.

In this section, the time-varying islanding operation is applied. According to the PV output and the load demand at each moment, the power supply areas of the islanding operation are dynamically changed, which facilitates to increase in the power supply reliability.

The type B in Figure 7 illustrates the time-varying islanding operation, which follows the following three principles:

1) At each moment, the total PV output should be larger than the total loads at all load points in the islanded network.

2) Starting from the load point where the PV system is integrated, the power supply of each load point is restored one by one from the shorter distance between each load point and PV system.

3) The power supply area of the islanding operation must be a connected domain.

Specifically, as shown in type B, the PV output during the first hour is larger than the total load demand of LP2 and LP3. Therefore, the power supply area is LP2 and LP3 during the first hour. In the second hour, the PV output becomes larger and can support larger load demand, i.e. LP2-LP4 during the second hour. During the N-th hour, the PV output becomes smaller, which can only supply the load at LP3, thus the power supply area is only LP3 during the N-th hour. The time-varying islanding operation can make full use of PV output to enhance the power supply reliability of distribution networks.

IV. DESIGN OF WHOLE ASSESSMENT PROCEDURE OF DISTRIBUTION NETWORK RELIABILITY

The whole assessment procedure of distribution network reliability is shown in Figure 8. The main steps in Figure 8 (a) are summarized and discussed as follows:

Step 1: Set the simulation time T and the precision e.

Step 2: Set the initial operation states of conventional power equipment to normal operation states, and the Time To Failure TTF is sampled using equation (24).

$$TTF = -\frac{1}{\lambda}\ln[U(0,\ 1)] \tag{24}$$

$$TTR = -\frac{1}{\mu}\ln[U(0,\ 1)] \tag{25}$$

The failure rate (λ) has been discussed in detail in Section II. In this paper, the maintenance rate (μ) is assumed to be the constant, and its probability distribution is assumed to be represented as the exponential distribution.

If the conventional power equipment is in failure state, the Time To Repair TTR is sampled using equation (25). On the other hand, if it is in normal operation state, the TTF is sampled.

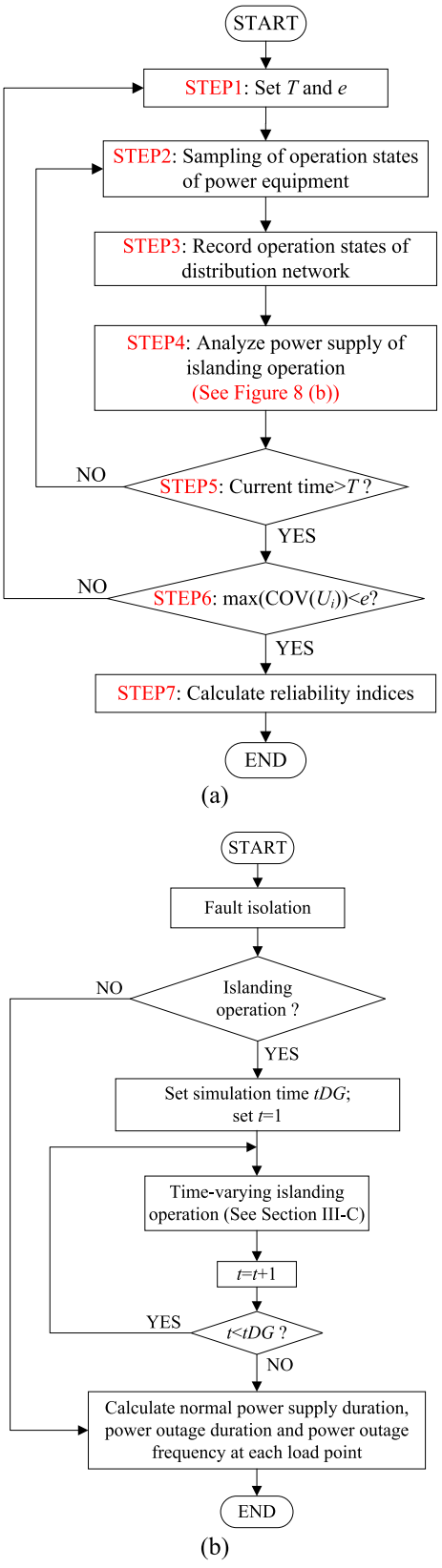

FIGURE 8. Whole assessment procedure of distribution network reliability. (a) Main steps of reliability assessment procedure. (b) Analysis of power supply during islanding operation.

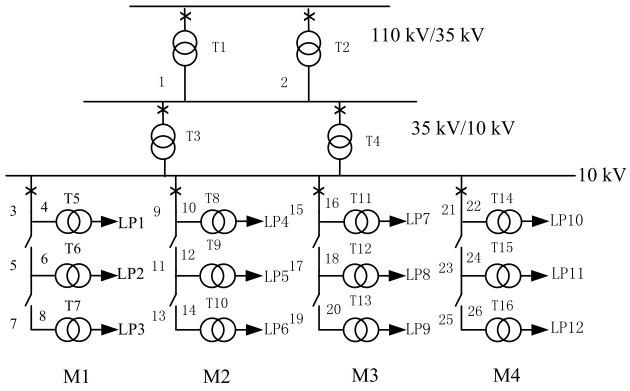

FIGURE 9. Distribution network topology in a region in China.

Step 3: According to *TTF* and *TTR* of each conventional power equipment, the time-varying operation states of distribution network are obtained.

Step 4: Analyze the power supply during the islanding operation, and the details are shown in Figure 8 (b). If there is the islanding operation, the PV output and the load at each moment are analyzed, and the power supply areas of the PV system are determined using the time-varying islanding operation.

The normal power supply duration, the power outage duration and the power outage frequency at each load point are calculated.

Step 5: If the current time reaches the simulation time T, go to Step 6; if not, go back to Step 2.

Step 6: Judge the convergence using equation (26). If the equation (26) is satisfied, go to Step 7; if not, go back to Step 1.

$$\max(COV(U_i)) \leq e \tag{26}$$

COV is the coefficient of variation.

$$COV \approx \sqrt{\hat{V}(F)/(S \cdot \hat{E}^2(F))} \tag{27}$$

Step 7: Calculate the reliability indices, such as APSTI, AESI, etc.

V. CASE STUDY

A. SIMULATION CONDITIONS

The topology of the studied distribution network is illustrated in Figure 9. This distribution network shows a radial network structure with several load points, which is a widely-used grid configuration in China. There are 50 conventional power equipment in the topology (26 feeders, 8 circuit breakers and 16 transformers). The circuit breakers are deployed at the supply end of feeders near the step-down transformers. Two isolating switches are deployed along each four main 10 kV feeder (M1, M2, M3, M4).

The load data at each load point is shown in Table 3. It can be seen that the loads on M1 feeder and M3 feeder are

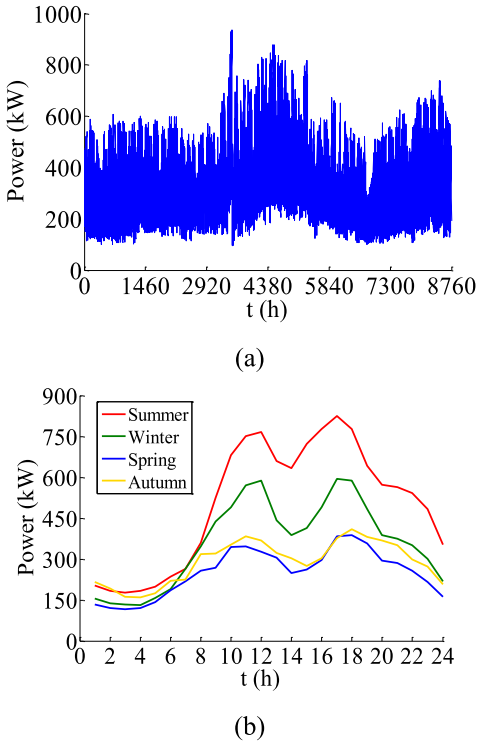

FIGURE 10. Time-varying load data of LP1. (a) Time-varying load data of LP1 in one year. (b) Time-varying load data of LP1 in four days in different seasons.

TABLE 3. Load data of distribution network.

Feeder	Load Point	Annual Peak Power (kW)	Number of Electricity Users	Mean Power (kW)
M1	LP1	936	2087	575
	LP2	1035	1601	636
	LP3	824	1534	506
M2	LP4	391	651	240
	LP5	315	914	193
	LP6	312	496	192
M3	LP7	1133	1195	696
	LP8	1057	1975	650
	LP9	830	1802	510
M4	LP10	503	1085	309
	LP11	516	887	317
	LP12	485	998	298

relatively larger. M1 and M3 have larger energy consumers, which leads to the annual peak power of over 800 kW at the load points on M1 and M3 feeders.

In order to reflect the time-varying load characteristics in this region, the time-varying load data at LP1 is shown in Figure 10. As shown in Figure 10 (a), the summer load is much higher than loads in other seasons, and the winter load is higher than spring and autumn ones. Figure 10 (b) reveals that the peak values of the four load curves in different seasons all appear around 10:00-12:00 and 17:00-19:00.

TABLE 4. Failure rates of model 1 and model 2.

Types	Failure Rates of Model 1	Failure Rates of Model 2
Feeder	0.046 (times/year·km)	0.046+0.0966 $t^{1.1}$ (times/year·km)
Transformer	0.015 (times/year)	0.015+0.0315 $t^{1.1}$ (times/year)
Circuit breaker	0.012 (times/year)	0.012+0.0252 $t^{1.1}$ (times/year)

TABLE 5. Comparison of reliability indices under different failure rate models.

	SAIFI (times/ household·year)	SAIDI (h/ household·year)	ENS (kWh/ year)
Model 1	2.74	9.51	34095
Model 2	3.97	13.63	48892
Difference	44.89%	43.32%	43.40%

B. INFLUENCE OF FAILURE RATE MODEL OF CONVENTIONAL POWER EQUIPMENT ON RELIABILITY ASSESSMENT

As discussed in Section II, most researches regard the failure rate of conventional power equipment (feeders, transformers, circuit breakers, etc.) as a constant. The model with the constant failure rate is called Model 1 here.

The failure rate model considering aging is called Model 2 here. The details of the time-varying failure rate model are discussed in Section II. For equation (2), setting that $\alpha_1 = \alpha_2$ and $\beta_2 = 2.1$. As discussed in [45], α_1 and α_2 are the constant failure rates under different conditions. If the influence of weather conditions (or other conditions) on the constant failure rate is ignored, α_1 can be regarded equal to α_2. $\beta_2(\beta_2 > 1)$ is the aging coefficient of failure rate, and the larger value depicts the faster aging process of the equipment.

The life cycles of feeders, transformers and circuit breakers are assumed to be 15 years, 20 years and 20 years, respectively. They are also assumed to start the aging periods in the 12th year, the 16th year and the 16th year, respectively.

The failure rates of Model 1 and Model 2 are shown in Table 4. In addition, the average maintenance time of feeders, transformers and breakers are set to 4 h, 50 h and 4 h, respectively.

Table 5 shows the reliability indices using Model 1 and Model 2. It can be seen that the SAIFI, the SAIDI and the ENS are all increased by more than 40% if the aging of conventional power equipment is considered. In other words, the failure rate model of conventional power equipment has a great impact on the reliability assessment. Therefore, the aging period of conventional power equipment cannot be ignored.

TABLE 6. Reliability indices under different PV integration positions.

Position	Conventional Reliability Indices					Newly Added Reliability Indices	
	SAIFI (times/ household ·year)	SAIDI (h/ household ·year)	CAIDI (h/ household· year)	ASAI (%)	ENS (kWh/ year)	APSTI (h/ year)	AESI (kWh/ year)
No PV	3.97	13.63	3.44	99.8444	48892	—	—
Supply End	3.98	13.41	3.37	99.8469	48062	3.85	1087
Middle Part	3.66	11.99	3.27	99.8632	43161	7.51	3790
Load End	3.54	11.55	3.26	99.8682	41824	11.45	4829
Maximum Difference	11.06%	15.26%	5.23%	0.02%	14.46%	66.38%	77.49%

TABLE 7. Reliability indices under different PV integration positions.

Position	Conventional Reliability Indices					Newly Added Reliability Indices	
	SAIFI (times/ household ·year)	SAIDI (h/ household ·year)	CAIDI (h/ household· year)	ASAI (%)	ENS (kWh/ year)	APSTI (h/ year)	AESI (kWh/ year)
No PV	3.97	13.63	3.44	99.8444	48892	—	—
M1	3.90	12.92	3.32	99.8525	46329	3.92	2032
M2	4.05	13.62	3.36	99.8445	48982	1.78	326
M3	3.91	13.00	3.32	99.8516	47054	3.26	1725
M4	4.00	13.39	3.35	99.8472	48120	2.66	774
Maximum Difference	3.70%	5.21%	3.49%	0.008%	5.42%	54.60%	84.00%

TABLE 8. Failure rates of different types of components in PV system.

	Transformer	Feeder	Inverter	PV Panel
Failure rate (times/year)	0.015	0.046	0.253	0.000133

TABLE 9. Reliability indices of characteristics of PV generations.

GRDG (%)	PIPDG (%)	PFDG (W/h)
19.52	46.13	94.18

C. COMPARISON OF CONVENTIONAL RELIABILITY INDICES AND NEWLY ADDED RELIABILITY INDICES

In order to compare the conventional reliability indices with the newly added reliability indices, the simulation scenario is set as follows:

It is assumed that the PV systems with the rated power of 2.5 MW are integrated to the supply ends, the middle parts and the load ends of four main feeders (M1, M2, M3, M4), respectively.

Table 6 shows the reliability indices of the aforementioned simulation scenario. It can be seen that the maximum differences of newly added reliability indices (APSTI and AESI) are all beyond 65%, while the maximum differences of conventional reliability indices (SAIFI, SAIDI, CAIDI, ASAI and ENS) are all below 16%. In other words, the sensitivity of newly added reliability indices is much higher than that of conventional reliability indices.

In order to further verify that the sensitivity of newly added reliability indices is indeed higher than that of conventional reliability indices, another simulation scenario is set as follows:

The PV system with the rated power of 2.5 MW is integrated to the load ends of four main feeders (M1, M2, M3, M4), respectively.

TABLE 10. Reliability indices under different PV output models.

	APSTI (h/ year)	AESI (kWh/ year)	SAIFI (times/ household·year)	SAIDI (h/ household·year)	ENS (kWh/year)
Model 1	10.72	4330	3.58	11.72	42411
Model2	10.33	4109	3.60	11.76	42603
Difference	-3.64%	-5.11%	0.56%	0.34%	0.45%

TABLE 11. Reliability indices under different islanding operation methods.

	APSTI (h/ year)	AESI (kWh/ year)
Model 1	11.29	2605.30
Model2	11.66	4948.11
Difference	3.28%	89.92%

TABLE 12. Penetration and rated power of PV system.

Penetration	5%	10%	20%	30%	40%	50%
Rated Power (kW)	416.9	833.8	1667.6	2501.4	3335.2	4169

The reliability indices of the aforementioned simulation scenario are shown in Table 7. It is seen that the maximum differences of the newly added reliability indices are all beyond 54% and the maximum difference of AESI is 84%, while the maximum differences of the conventional reliability indices are all below 6%. Thus, it can be concluded that the sensitivity of the newly added reliability indices is much higher than that of the conventional reliability indices.

The reason why the sensitivity of the conventional reliability indices is worse than that of the newly added reliability indices is as follows:

The calculation of SAIFI, SAIDI, ASAI, CAIFI, CAIDI, ENS involves all the load points in the distribution network. In other words, when the PV output cannot cover the loads at all load points in the whole distribution network, the sensitivity of reliability changes will be diluted by the load points where the PV output cannot restore. However, the calculation of APSTI and AESI only focuses on the power supply area of the islanding operation (i.e., R_j in equations (14)-(15)), and the reliability changes can be more sensitively reflected, which is more proper to assess the power supply reliability during the islanding operation.

The reliability indices for power equipment, i.e. the failure rate (λ) and the maintenance rate (μ) are used to calculate *TTF* and *TTR* (applying equations (24) and (25)), and then the situation of the system failure can be obtained. In the context of available reliability indices for power equipment, the nature of APSTI and AESI is to describe the power supply reliability from the perspective of time and energy, which is consistent with the description for power supply reliability from the conventional perspective.

D. INFLUENCE OF PV OUTPUT MODEL ON RELIABILITY ASSESSMENT OF POWER SUPPLY OF ISLANDING OPERATION

The simulation of radiation intensity in this region is performed using the kernel density estimation. Figure 11 shows the simulation result of the annual radiation intensity. It can be seen that the accuracy is high.

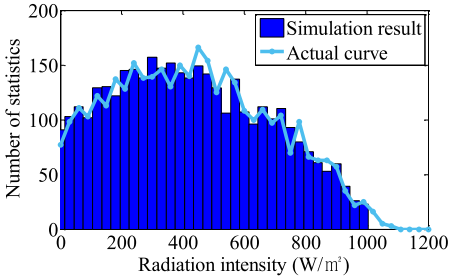

FIGURE 11. Simulation result of radiation intensity.

The failure rates of different types of components in PV system are shown in Table 8. It is assumed that the life cycle of PV system is 20 years. The first 15 years are the stabilization period of each component, and the failure rate is treated as constant. The last 5 years are the aging period of each component, and the equation (2) is applied to calculate the failure rates.

GRDG, PIPDG and PFDG of the PV system with the rated power of 1.5 MW are shown in Table 9. The GRDG, PIPDG and PFDG quantitatively reflect the characteristics of the PV output in this region. The case studies in this paper are based on the following characteristics of PV output: the PV generation rate of nearly 20% with relative to the rated values, the PV output interruption probability of nearly 50%, and the deviation of PV output of nearly 0.1 kW/h.

In order to analyze the influence of PV output model on reliability assessment during islanding operation. It is assumed that the PV systems with the rated power of 1.5 MW are connected to the load ends of the four main feeders. Two different PV output models are set as follows.

Model 1: PV output model without consideration of the failure and the degradation of PV modules.

Model 2: PV output model considering the failure and the degradation of PV modules.

The reliability indices using the two PV output models are shown in Table 10.

As seen in Table 10, the differences of APSTI and AESI under the two PV output models are obvious: the APSTI

TABLE 13. Reliability indices under different PV penetration and different methods.

Penetration level	APSTI (h/year)			AESI (kWh/ year)		
	Procedure 1	Procedure 2	Difference	Procedure 1	Procedure 2	Difference
5%	3.75	5.13	36.8%	588	1437	144.39%
10%	6.36	8.69	36.64%	1276	3175	148.82%
20%	7.88	10.97	39.21%	1764	4500	155.10%
30%	8.20	11.60	41.46%	1900	4852	155.37%
40%	8.66	11.84	36.72%	2009	5051	151.42%
50%	8.72	12.09	38.65%	2053	5172	151.92%

decreases by 3.64% and the AESI decreases by 5.11%. The reason for the difference of APSTI and AESI is the additional consideration of the failure and the degradation of PV modules in the proposed PV output model, which is unignorable. While, the deviation of SAIFI, SAIDI and ENS are merely 0.56%, 0.34% and 0.45%, respectively. The results also indicate that APSTI and AESI are more suited for the reliability assessment during islanding operation when PV systems are connected to the distribution network.

E. INFLUENCE OF ISLANDING OPERATION METHOD ON RELIABILITY ASSESSMENT OF POWER SUPPLY

In order to analyze the influence of islanding operation method on reliability assessment, the 2.5 MW PV systems are assumed to be integrated at the load ends of the four main feeders. The two islanding operation methods are set as follows:

Method 1: the power supply areas of islanding operation are fixed to the load points with PV power integration.

Method 2: based on the time-varying PV output and load demand at each moment, the power supply areas of islanding operation are dynamically changed.

Table 11 shows the reliability indices under the two islanding operation methods. It is seen that the difference of AESI under the two islanding operation methods is up to 89.92%. In other words, the islanding operation method has a great impact on the power supply reliability.

F. INFLUENCE OF WHOLE ASSESSMENT PROCEDURE ON RELIABILITY ASSESSMENT

In order to analyze the influence of the whole assessment procedure on the reliability assessment, the two different assessment procedures are shown as follows:

Procedure 1: the failure rate of conventional power equipment is assumed to be constant; the failure and the degradation of PV modules are ignored in PV output modelling; the power supply areas of islanding operation are fixed.

Procedure 2: the aging of conventional power equipment is considered and the time-varying failure rate model is applied; the aging of PV modules is considered and the PV output model with consideration of the failure and the degradation of PV modules is applied; the time-varying islanding operation is applied.

It is assumed that the load ends of the four main feeders (M1, M2, M3, M4) are all integrated with PV systems to improve the power supply reliability. According to the averaged load in Table 3, the rated power of PV system under the different penetration levels is calculated as shown in Table 12.

Table 13 shows the calculation results of reliability indices under the different PV penetration levels using Procedures 1 and 2. It can be seen that the influence of the whole assessment procedure on APSTI is more than 35%, and the influence of the whole assessment procedure on AESI is up to more than 140%. The results in Table 13 indicate that when the negative influences of the following unreasonable situations are overlapped, accuracy of reliability assessment result could be significantly decreased.

(1) Unreasonable failure rate model without considering the aging.

(2) Unreasonable PV output model without considering the failure and the degradation of PV modules.

(3) Unreasonable islanding operation method without considering the dynamic change in the power supply area of the PV system.

VI. CONCLUSION

In order to accurately assess the power supply reliability in the distribution network with PVs, a reliability assessment procedure of the distribution network was proposed.

Firstly, the failure rate model of conventional power equipment was cultivated considering aging period. This contributed to more accurate assessment of the negative impact of system faults on reliability.

Then, three items were devised to accurately evaluate the reliability improvement in distribution grids with the PV: 1) Newly added five reliability indices increased the sensitivity for the reliability change during islanding operation. 2) The PV output model considering aging processes (failure and degradation of PV modules) enabled the modelling of more realistic PV output. 3) The time-varying islanding operation in the distribution network with PVs was incorporated in a reliability assessment procedure.

Finally, the whole assessment procedure was designed.

The case studies using the real-life distribution network topology in China revealed the following results:

(1) When it comes to the influence of the failure rate model of conventional power equipment on reliability assessment;

the assessment result was impacted more than 40% without the aging process of conventional power equipment.

(2) The maximum differences of newly added reliability indices were all beyond 50%, which were more obvious than that of conventional reliability indices (lower than 16%). In other words, the newly added reliability indices show more sensitivity.

The failure and degradation of PV modules showed an impact on the reliability assessment of power supply of islanding operation, which cannot be ignored.

The reliability, using time-vayring islanding operation, was nearly 90% higher than the time-invariant islanding operation, which indicated that the time-varying islanding operation was much more logical compared to the time-invariant islanding operation.

(3) It is noted that the influence of whole assessment procedure on reliability assessment was nearly 150%. It can be seen that the unreasonable reliability assessment procedure will have a huge impact on the reliability assessment.

Overall, the unreasonable reliability assessment procedure can take the results away from the reality. The accuracy of reliability assessment will produce a crucial impact on the system operation and planning.

Although the current study shows the outstanding contributions, the following work still remains:

Analysis of the power supply reliability in the distribution network with other types of distributed source integration will be conducted.

The debugging period of conventional power equipment will be analyzed to establish more tailored failure rate models.

The different maintenance time span under different maintenance strategies will be studied.

REFERENCES

[1] F. Wang, H. Xu, T. Xu, K. Li, M. Shafie-Khah, and J. P. Catalão, "The values of market-based demand response on improving power system reliability under extreme circumstances," *Appl. Energy*, vol. 193, pp. 220–231, May 2017.

[2] S. Su *et al.*, "Research on an electric vehicle owner-friendly charging strategy using photovoltaic generation at office sites in major Chinese cities," *Energies*, vol. 11, no. 2, p. 421, Feb. 2018.

[3] A. Escalera, B. Hayes, and M. Prodanović, "A survey of reliability assessment techniques for modern distribution networks," *Renew. Sustain. Energy Rev.*, vol. 91, pp. 344–357, Aug. 2018.

[4] Z.-J. Liu, G.-H. Wu, D.-H. Yin, and Q. Song, "Reliability assessment of distribution network considering the randomness of distributed generation," in *Proc. China Int. Conf. Electr. Distrib.*, Xi'an, China, Aug. 2016, pp. 1–6.

[5] N. Z. Xu and C. Y. Chung, "Reliability evaluation of distribution systems including vehicle-to-home and vehicle-to-grid," *IEEE Trans. Power Syst.*, vol. 31, no. 1, pp. 759–768, Jan. 2016.

[6] S. Conti, S. A. Rizzo, E. F. El-Saadany, M. Essam, and Y. M. Atwa, "Reliability assessment of distribution systems considering telecontrolled switches and microgrids," *IEEE Trans. Power Syst.*, vol. 29, no. 2, pp. 598–607, Mar. 2014.

[7] J. Zhong, W. Li, C. Wang, J. Yu, and R. Xu, "Determining optimal inspection intervals in maintenance considering equipment aging failures," *IEEE Trans. Power Syst.*, vol. 32, no. 2, pp. 1474–1482, Mar. 2017.

[8] J. Wang, X. Xiong, N. Zhou, Z. Li, and S. Weng, "Time-varying failure rate simulation model of transmission lines and its application in power system risk assessment considering seasonal alternating meteorological disasters," *IET Gener., Transmiss. Distrib.*, vol. 10, no. 7, pp. 1582–1588, May 2016.

[9] *IEEE Guide for Electric Power Distribution Reliability Indices*, IEEE Standard 1366, 2012.

[10] H. Bai, S. Miao, P. Zhang, and Z. Bai, "Reliability evaluation of a distribution network with microgrid based on a combined power generation system," *Energies*, vol. 8, no. 2, pp. 1216–1241, Feb. 2015.

[11] A. R. Abul'Wafa and A. T. M. Taha, "Reliability evaluation of distribution systems under μ grid-tied and Islanded μ grid modes using Monte Carlo simulation," *Smart Grid Renew. Energy*, vol. 5, no. 3, pp. 52–62, Mar. 2014.

[12] D.-L. Duan, X.-D. Ling, X.-Y. Wu, and B. Zhong, "Reconfiguration of distribution network for loss reduction and reliability improvement based on an enhanced genetic algorithm," *Int. J. Elect. Power Energy Syst.*, vol. 64, pp. 88–95, Jan. 2015.

[13] Y. Wang, "Analytical complex distribution system reliability evaluation considering stochastic interruption durations and network reconfigurations," *Electr. Power Compon. Syst.*, vol. 45, no. 19, pp. 2151–2163, Feb. 2018.

[14] A. A. Hourani and M. Almuhaini, "Impact of demand side management on the reliability performance of power distribution systems," in *Proc. Saudi Arabia Smart Grid*, Jeddah, Saudi Arabia, Dec. 2016, pp. 1–5.

[15] H. Wang, H. Lin, T. Yu, Z. Xu, and Y. Mishra, "Dynamic equivalent-based reliability evaluation of distribution systems with DGs," *IET Gener., Transmiss. Distrib.*, vol. 10, no. 10, pp. 2285–2294, Jul. 2016.

[16] G. Li, Z. Bie, H. Xie, and Y. Lin, "Customer satisfaction based reliability evaluation of active distribution networks," *Appl. Energy*, vol. 162, pp. 1571–1578, Jan. 2016.

[17] G. Li, Z. Bie, H. Xie, X. Wang, and X. Wang, "Reliability evaluation of active distribution networks considering customer satisfaction," *Energy Procedia*, vol. 61, pp. 591–594, Jan. 2014.

[18] Z. H. Bie, G. F. Li, and H. P. Xie, "Reliability evaluation of microgrids considering coordinative optimization of loads and storage devices," *Trans. China Electrotech. Soc.*, vol. 29, no. 2, pp. 64–73, Feb. 2014.

[19] M. A. Abdullah, A. P. Agalgaonkar, and K. M. Muttaqi, "Assessment of energy supply and continuity of service in distribution network with renewable distributed generation," *Appl. Energy*, vol. 113, pp. 1015–1026, Jan. 2014.

[20] M. Q. Raza, M. Nadarajah, and C. Ekanayake, "On recent advances in PV output power forecast," *Sol. Energy*, vol. 136, pp. 125–144, Oct. 2016.

[21] J.-K. Park, A. Das, and J.-H. Park, "A new approach to estimate the spatial distribution of solar radiation using topographic factor and sunshine duration in South Korea," *Energy Convers. Manage.*, vol. 101, pp. 30–39, Sep. 2015.

[22] L. M. Aguiar, B. Pereira, M. David, F. Díaz, and P. Lauret, "Use of satellite data to improve solar radiation forecasting with Bayesian artificial neural networks," *Sol. Energy*, vol. 122, pp. 1309–1324, Dec. 2015.

[23] A. Linares-Rodriguez, J. A. Ruiz-Arias, D. Pozo-Vazquez, and J. Tovar-Pescador, "An artificial neural network ensemble model for estimating global solar radiation from Meteosat satellite images," *Energy*, vol. 61, no. 6, pp. 636–645, Nov. 2013.

[24] D. Laslett, C. Creagh, and P. Jennings, "A method for generating synthetic hourly solar radiation data for any location in the south west of Western Australia, in a world wide Web page," *Renew. Energy*, vol. 68, pp. 87–102, Aug. 2014.

[25] W. Yao, Z. Li, Y. Wang, F. Jiang, and L. Hu, "Evaluation of global solar radiation models for Shanghai, China," *Energy Convers. Manage.*, vol. 84, pp. 597–612, Aug. 2014.

[26] M. A. Shamim, R. Remesan, M. Bray, and D. Han, "An improved technique for global solar radiation estimation using numerical weather prediction," *J. Atmos. Sol.-Terr. Phys.*, vol. 129, pp. 13–22, Jul. 2015.

[27] A. Dumas *et al.*, "A new correlation between global solar energy radiation and daily temperature variations," *Sol. Energy*, vol. 116, pp. 117–124, Jun. 2015.

[28] Z. Ren, W. Yan, X. Zhao, W. Li, and J. Yu, "Chronological probability model of photovoltaic generation," *IEEE Trans. Power Syst.*, vol. 29, no. 3, pp. 1077–1088, May 2014.

[29] Y. Zhang and J. Wang, "GEFCom2014 probabilistic solar power forecasting based on k-nearest neighbor and kernel density estimator," in *Proc. IEEE Power Energy Soc. Gen. Meeting*, Denver, CO, USA, Jul. 2015, pp. 1–5.

[30] T. Yamazaki, H. Homma, S. Wakao, Y. Fujimoto, and Y. Hayashi, "Estimation prediction interval of solar irradiance based on just-in-time modeling for photovoltaic output prediction," *Elect. Eng. Jpn.*, vol. 135, no. 3, pp. 160–167, Mar. 2015.

[31] T. Lai, R. Biggie, A. Brooks, B. G. Potter, and K. Simmons-Potter, "Environmental aging in polycrystalline-Si photovoltaic modules: Comparison of chamber-based accelerated degradation studies with field-test data," *Proc. SPIE*, vol. 9563, Sep. 2015, Art. no. 956309.
[32] D. A. Quansah and M. S. Adaramola, "Ageing and degradation in solar photovoltaic modules installed in northern Ghana," *Sol. Energy*, vol. 173, pp. 834–847, Oct. 2018.
[33] Q. Li and F. H. Khan, "Identifying natural degradation/aging in power MOSFETs in a live grid-tied PV inverter using spread spectrum time domain reflectometry," in *Proc. Int. Power Electron. Conf.*, Hiroshima, Japan, May 2014, pp. 2161–2166.
[34] M. Mosadeghy, R. Yan, and T. K. Saha, "A time-dependent approach to evaluate capacity value of wind and solar PV generation," *IEEE Trans. Sustain. Energy*, vol. 7, no. 1, pp. 129–138, Jan. 2016.
[35] T. Fan, S. Du, K. Liu, J. Su, and Y. Liu, "Reliability evaluation based on Monte Carlo simulation considering islanded operation in distribution network with micogrid," in *Proc. Int. Conf. Renew. Power Gener.*, Beijing, China, Oct. 2015, pp. 1–6.
[36] K. Zou, A. P. Agalgaonkar, K. M. Muttaqi, and S. Perera, "An analytical approach for reliability evaluation of distribution systems containing dispatchable and nondispatchable renewable DG units," *IEEE Trans. Smart Grid*, vol. 5, no. 6, pp. 2657–2665, Nov. 2014.
[37] S. Conti and S. A. Rizzo, "Monte Carlo simulation by using a systematic approach to assess distribution system reliability considering intentional islanding," *IEEE Trans. Power Del.*, vol. 30, no. 1, pp. 64–73, Feb. 2015.
[38] H. Guo, V. Levi, and M. Buhari, "Reliability assessment of smart distribution networks," in *Proc. IEEE Innov. Smart Grid Technol.-Asia*, Bangkok, Thailand, Nov. 2015, pp. 1–6.
[39] C. L. T. Borges and M. Costa, "Reliability assessment of microgrids with renewable generation by an hybrid model," in *Proc. IEEE Eindhoven PowerTech*, Eindhoven, The Netherlands, Jun. 2015, pp. 1–6.
[40] A. Heidari, V. G. Agelidis, H. Zayandehroodi, J. Pou, and J. Aghaei, "On exploring potential reliability gains under islanding operation of distributed generation," *IEEE Trans. Smart Grid*, vol. 7, no. 5, pp. 2166–2174, Sep. 2016.
[41] X. Xiang, Y. Yue, W. Zou, and Z. Li, "Reliability evaluation of microgrid power supply in emergency non-scheduled isolated mode," *Automat. Electr. Power Syst.*, vol. 36, no. 9, pp. 18–23, May 2012.
[42] Z. Liu, X. Wang, R. Zhuo, and X. Cai, "Flexible network planning of autonomy microgrid," *IET Renew. Power Gener.*, vol. 12, no. 16, pp. 1931–1940, Dec. 2018.
[43] Y. Luo, L. Wang, G. Zhu, and G. Wang, "Network analysis and algorithm of microgrid reliability assessment," in *Proc. Asia–Pacific Power Energy Eng. Conf.*, Chengdu, China, Mar. 2010, pp. 1–4.
[44] T.-Y. Chen, W.-T. Lin, and S. Chwen, "A dynamic failure rate forecasting model for service parts inventory," *Sustainability*, vol. 10, no. 7, p. 2408, Jul. 2018.
[45] D. Duan, X. Wu, and H. Deng, "Reliability evaluation of distribution systems based on time-varying failure rate and service restoration time model," *Proc. Chin. Soc. Elect. Eng.*, vol. 31, no. 28, pp. 57–64, Oct. 2011.
[46] L. Li, X. Xiao, and P. Chen, "Improved photovoltaic model and its application in reliability evaluation of micro-grid," *Adv. Technol. Elect. Eng. Energy*, vol. 35, no. 11, pp. 65–71, Nov. 2016.
[47] M. Vázquez and I. Rey-Stolle, "Photovoltaic module reliability model based on field degradation studies," *Prog. Photovolt. Res. Appl.*, vol. 16, no. 5, pp. 419–433, Aug. 2008.

SU SU received the M.Eng. and Ph.D. degrees in electrical engineering from Tohoku University, Japan, in 2006 and 2009, respectively.

Since 2011, she has been an Associate Professor with the School of Electrical Engineering, Beijing Jiaotong University. Her current research interests include reliability assessment of active distribution network, vehicle-to-grid (V2G) energy management, optimal and economic dispatching of renewable energy generations, and intelligent energy management of electric vehicles considering users' cognitive characteristics.

YONG HU received the B.Eng. degree in electrical engineering and automation from the Agricultural University of Hebei, Baoding, Hebei, China, in 2014, and the M.Eng. degree in electrical engineering from Beijing Jiaotong University, Beijing, China, in 2017.

His current research interests include power system stability analysis, power supply reliability of distribution networks, optimal operation and planning of power system with renewable energy or electric vehicles integration, and electric vehicles coordinated charging strategies.

LUOBIN HE received the B.Eng. degree in electrical engineering and automation and the M.Eng. degree in electrical engineering from Beijing Jiaotong University, Beijing, China, in 2015 and 2018, respectively.

She is currently a Teacher with the Department of Electrical Engineering, Hunan Polytechnic of Water Resources and Electric Power. Her research interests include the reliability assessment of distribution network with renewable energy integration, and the optimal dispatching of renewable energy generations.

KOJI YAMASHITA received the B.S. and M.S. degrees in electrical engineering from Waseda University, Tokyo, Japan, in 1993 and 1995, respectively. He is currently pursuing the Ph.D. degree with Michigan Technological University.

He has been a Senior Research Scientist with the Central Research Institute of Electric Power Industry, Tokyo, since 1995. He was a Visiting Researcher with Iowa State University, from 2006 to 2007. His areas of interest include power system dynamics, wide-area protection and, control, and cybersecurity; as well as generation/load modeling including renewable energy sources, electric vehicles, and energy storage systems. He is a member of the CIGRE and the Institute of Electrical Engineers of Japan.

SHIDAN WANG received the B.Eng. degree in electrical engineering and automation from the South China University of Technology, Guangzhou, Guangdong, China, in 2010, and the M.Eng. degree in electrical engineering from Beijing Jiaotong University, Beijing, China, in 2012.

He is currently engaged in relay protection related work with State Grid Beijing Haidian Electric Power Supply Company. His research interest mainly focuses on reactive power optimization in power systems.